Optics Letters

Generation of narrowband, high-intensity, carrier-envelope phase-stable pulses tunable between 4 and 18 THz

B. Liu,[1] H. Bromberger,[1] A. Cartella,[1] T. Gebert,[1] M. Först,[1,*] and A. Cavalleri[1,2]

[1]Max Planck Institute for the Structure and Dynamics of Matter, Hamburg, Germany
[2]Department of Physics, Oxford University, Clarendon Laboratory, Parks Road, Oxford, UK
*Corresponding author: michael.foerst@mpsd.mpg.de

Received 24 October 2016; revised 24 November 2016; accepted 5 December 2016; posted 6 December 2016 (Doc. ID 279310); published 23 December 2016

We report on the generation of high-energy (1.9 μJ) far-infrared pulses tunable between 4 and 18 THz frequency. Emphasis is placed on tunability and on minimizing the bandwidth of these pulses to less than 1 THz, as achieved by difference-frequency mixing of two linearly chirped near-infrared pulses in the organic nonlinear crystal DSTMS. As the two near-infrared pulses are derived from amplification of the same white light continuum, their carrier envelope phase fluctuations are mutually correlated, and hence the difference-frequency THz field exhibits absolute phase stability. This source opens up new possibilities for the control of condensed matter and chemical systems by selective excitation of low-energy modes in a frequency range that has, to date, been difficult to access.

OCIS codes: (190.7110) Ultrafast nonlinear optics; (160.4890) Organic materials; (050.1590) Chirping; (120.5050) Phase measurement.

https://doi.org/10.1364/OL.42.000129

Fingerprints of many important phenomena in life sciences, chemistry, and solid-state physics are found at terahertz frequencies. These features are conveniently probed with conventional spectrometers powered by lamps or synchrotron radiation. However, a number of important experimental works aim at studying the response of matter to strong fields as a tool for nonlinear spectroscopy or as a means of optical control.

For example, recent experiments have demonstrated the control of the functional electronic and magnetic properties of certain complex solids through the direct optical excitation of low-energy vibrational modes [1]. In particular, strong optical pulses at mid-infrared frequencies have been used to coherently drive and control insulator-metal transitions [2], magnetization dynamics [3], as well as to induce transient superconducting states far above equilibrium transition temperatures in high-T_C superconductors [4,5]. Yet, the lack of powerful sources with frequencies <15 THz has restricted this selective control to a particular set of higher-energy vibrational modes in these materials.

Free-electron lasers do provide high-energy pulses at frequencies below 20 THz [6], although these are typically of several-picoseconds duration and do not possess carrier-envelope phase (CEP) stability.

Tabletop femtosecond lasers are the most versatile tool to generate and measure high-intensity radiation throughout this frequency region. Transient electric fields of 1 MV/cm have been achieved below 3 THz frequency by optical rectification of pulse-front-tilted near-infrared pulses in $LiNbO_3$ [7]. Difference-frequency generation (DFG) in GaSe nonlinear crystals has been shown to generate ~100 MV/cm phase-locked tunable electric fields at mid-infrared frequencies, limited to frequencies above 15 THz due to strong absorption and dispersion found at the Reststrahlen band of the material [8,9].

Recently, the availability of large organic crystals, which exhibit significant nonlinear susceptibility and low absorption in the THz range, has opened up new possibilities [10–15]. For example, broadband continuum generation up to 15 THz has been demonstrated through optical rectification in HMQ-TMS [11]. Also, sub-mJ THz pulses tunable up to 7 THz with selectable spectral bandwidth have been generated by optical rectification of temporally modulated, chirped near-infrared laser pulses in a DSTMS [13]. On the other hand, narrowband nanojoule THz pulses widely tunable between 1 and 20 THz were produced by difference-frequency mixing signal and idler beams from nanosecond optical parametric oscillators in a DAST organic crystal [14].

In this Letter, we present one suitable scheme to generate narrowband far-infrared pulses utilizing DFG between two chirped near-infrared pulses in a DSTMS organic crystal. Sub-picosecond pulses tunable between 4 and 18 THz are demonstrated, with a bandwidth of less than 1 THz (FWHM). A key element of this scheme is the use of stretched near-IR pulses, which is crucial to suppress the emission of broadband low-frequency (<4 THz) radiation. A maximum pulse energy of 1.9 μJ is achieved, resulting in a peak electric field and peak intensity of 3.7 MV/cm and 17.8 GW/cm^2, respectively.

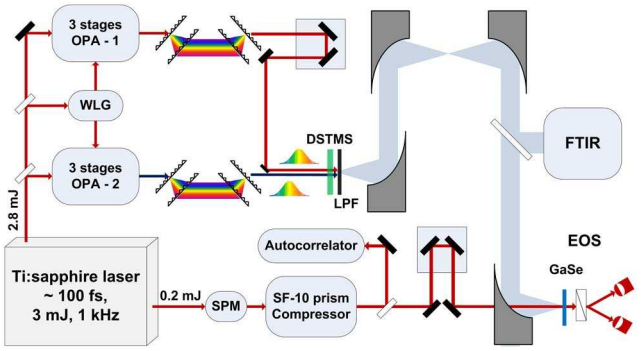

Fig. 1. Narrowband THz setup. A Ti:sapphire regenerative amplifier serves to pump two separate three-stage optical parametric amplifiers seeded by the same white-light continuum. The signal output pulses, tuned between 1.35 and 1.5 μm wavelength, are linearly chirped by sets of high-efficiency transmission gratings and used for the DFG process in the DSTMS nonlinear crystal. The generated THz electric fields are characterized via FTIR or via electro-optic sampling in a GaSe crystal, the latter using ~50 fs gate pulses.

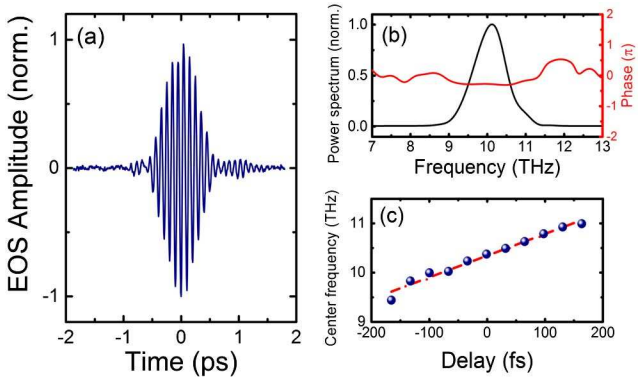

Fig. 2. (a) THz transient electric field generated by DFG in a 480 μm thick DSTMS crystal as detected via electro-optic sampling in a GaSe crystal of 100 μm thickness. (b) Corresponding power spectrum (black) and spectral phase (red). (c) Center frequency of the THz transient as a function of the time delay between two near-IR signal pulses. The red dash-dotted line is a linear fit.

Figure 1 displays a schematic drawing of the optical setup used in this study. A commercial Ti:sapphire regenerative amplifier, delivering 800 nm wavelength pulses of 3 mJ energy and ~100 fs duration at 1 kHz repetition rate was used to pump two identical three-stage optical parametric amplifiers (OPA). These OPAs were seeded by the same white light continuum, in order to generate pulses with correlated carrier-envelope phase fluctuations that could then be subtracted in the DFG process [16], hence yielding a stable carrier-envelope phase of the THz radiation [8,9]. Each OPA generated signal output pulses of maximum ~380 μJ energy and ~130 fs duration, which were tuned between 1.35 and 1.5 μm. The near-IR beams were collimated to diameters of about 2 mm, keeping the fluence incident on the DSTMS crystal below its damage threshold of 150 GW/cm^2. Efficient DFG in the nonlinear DSTMS crystal requires type-0 phase matching, facilitated by polarizing both near-IR beams along to the crystal *a* axis and choosing a quasi-collinear geometry with <0.1° angle [15].

Two pulse stretchers, each built from four high-efficiency transmission gratings (~95% diffraction efficiency between 1.4 and 1.55 μm), were used to introduce equivalent amounts of negative linear chirp to the near-IR pulses. As a consequence, two frequency combs with a single beating frequency propagate through the nonlinear DSTMS crystal to produce the THz electric fields. The beating frequency could then be tuned by changing the delay between the near-infrared pulses. Stretching to about 600 fs was chosen for these experiments, to suppress the coherent THz emission from optical rectification while retaining enough field strength for efficient difference frequency generation [17,18].

The generated THz fields were transmitted through three 20-THz low-pass filters (QMC Instruments) to block the residual near-infrared beams and characterized by either Fourier-transform interference (FTIR) or electro-optic sampling in a 100 μm thick GaSe crystal. For the latter, ~50 fs gating pulses were obtained by spectral broadening and compression of a low-energy replica of the fundamental 800 nm beam, using a thin sapphire crystal and a prism compressor (SF-10).

Figure 2(a) shows an electro-optic sampling measurement of a CEP-stable THz electric field generated in a 480 μm thick DSTMS crystal by mixing two OPA signal wavelengths tuned to 1430 and 1500 nm, respectively. The THz pulse duration calculated from these data is ~420 fs (FWHM). The corresponding power spectrum, plotted in Fig. 2(b) together with its flat spectral phase, is centered at 10 THz and shows a <1 THz bandwidth. The center frequency is in agreement with the difference of the two generating near-IR frequencies of 209.6 and 199.8 THz.

The long-term stability of the phase of the electric field was measured by consecutively sampling the THz pulses. Within four hours, the phase accumulated a linear drift of 0.14π with residual fluctuations of 0.03π (standard deviation). These instabilities are likely due to thermal and mechanical fluctuations in the optical setup and could be further reduced by implementing an active stabilization scheme as described in Ref. [9].

The pulse energy of the electric field transient shown above, measured by a commercial thermopile detector (Ophir Optronics, Model 3A-P-THz), was 1.9 μJ. Two parabolic mirrors were used to first collimate and then focus the THz beam onto the electro-optic detection crystal. A spot size of 180 μm was determined from knife-edge measurements, resulting in a peak electric field of 3.7 MV/cm ($E_{\text{peak}} = \sqrt{2Z_0 W_{\text{pulse}}/A_{\text{pulse}}\,\tau_{\text{pulse}}}$ with Z_0 the vacuum impedance; W_{pulse}, A_{pulse}, and t_{pulse} the energy, area, and duration of the THz pulse). The corresponding peak intensity was 17.8 GW/cm^2.

Fine tuning of the THz center frequency was possible by delaying these pulses with respect to each other, as illustrated in Fig. 2(c). Furthermore, the THz pulse duration and bandwidth were continuously tunable by adjusting the amount of linear chirp in the grating stretcher, limited however by the onset of optical rectification for short pulses as well as low peak intensities in the DFG process for long pulses.

The center frequency of the THz fields could be further tuned by adjusting the center wavelengths of the two mixing near-IR beams. For the collinear geometry used here, the condition for type-0 phase matching is determined by the dispersion of the refractive index along the crystallographic *a*

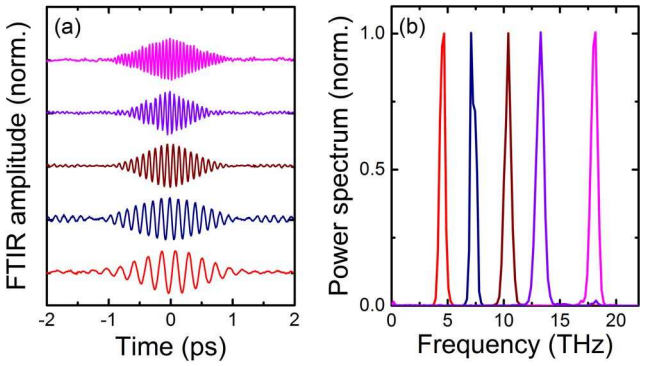

Fig. 3. Normalized (a) FTIR interferograms and (b) corresponding Fourier transformations of THz transient electric fields, tuned by changing the difference frequency between the two linearly chirped near-IR pulses.

axis, which in the organic DSTMS crystal comprises vibrational resonances at THz frequencies [19]. Therefore, satisfying the phase matching conditions for a desired THz output frequency was not only sensitive to the difference in the near-infrared photon energies, but also to the frequencies themselves [14]. This is in contrast to type-I or type-II phase matching in, e.g., GaSe, which are typically used to produce >15 THz pulses. In these crystals, the refractive index dispersion is relatively flat and the DFG frequencies can be chosen rather arbitrarily.

Figure 3(a) shows FTIR traces of electric field transients tuned across a broad spectral range below 20 THz. The corresponding Fourier transforms, shown in Fig. 3(b), confirm the tunability of the developed source between about 4 and 18 THz. To achieve maximum pulse energy at a desired THz frequency the center wavelengths of the two near-infrared pulses were tuned simultaneously. For example, 4.5 THz pulses were generated by mixing two signal wavelengths at 1395 and 1425 nm. The amount of chirp on the two near-IR pulses was kept constant throughout these measurements, resulting in spectral bandwidths always below 1 THz. The pulse energy for these different frequencies varies between 1.3 and 1.9 μJ, likely due to the frequency-dependent absorption coefficient of the DSTMS crystal [19].

We note that the present source might be extended to both lower and higher frequencies, as 1–20 THz tunability has been demonstrated earlier in an organic crystal-based nanosecond-pulsed DFG setup [14].

In summary, we reported a tabletop source of narrowband, high-intensity, carrier-envelope-stable far-infrared electromagnetic fields, tunable between 4 and 18 THz. Pulse energies of up to ~2 μJ with peak electric field of >3.5 MV/cm were demonstrated when pumping the system with 3 mJ pulses from a Ti:sapphire regenerative amplifier. Chirping the two near-IR pulses used in the THz-generating difference frequency mixing process is crucial to suppress broadband THz radiation otherwise generated via optical rectification. We predict this system to be scalable to higher intensities by increasing the 800 nm pulse energy and adapting spot sizes throughout the whole chain of involved nonlinear processes.

REFERENCES

1. M. Först, C. Manzoni, S. Kaiser, Y. Tomioka, Y. Tokura, R. Merlin, and A. Cavalleri, Nat. Phys. **7**, 854 (2011).
2. M. Rini, R. Tobey, N. Dean, J. Itatani, Y. Tomioka, Y. Tokura, R. W. Schoenlein, and A. Cavalleri, Nature **449**, 72 (2007).
3. M. Först, A. D. Caviglia, R. Scherwitzl, R. Mankowsky, P. Zubko, V. Khanna, H. Bromberger, S. B. Wilkins, Y.-D. Chuang, W. S. Lee, W. F. Schlotter, J. J. Turner, G. L. Dakovski, M. P. Minitti, J. Robinson, S. R. Clark, D. Jaksch, J.-M. Triscone, J. P. Hill, S. S. Dhesi, and A. Cavalleri, Nat. Mater. **14**, 883 (2015).
4. D. Fausti, R. I. Tobey, N. Dean, S. Kaiser, A. Dienst, M. C. Hoffmann, S. Pyon, T. Takayama, H. Takagi, and A. Cavalleri, Science **331**, 189 (2011).
5. M. Mitrano, A. Cantaluppi, D. Nicoletti, S. Kaiser, A. Perucchi, S. Lupi, P. Di Pietro, D. Pontiroli, M. Riccò, S. R. Clark, D. Jaksch, and A. Cavalleri, Nature **530**, 461 (2016).
6. S. A. Zvyagin, M. Ozerov, E. Čižmár, D. Kamenskyi, S. Zherlitsyn, T. Herrmannsdörfer, J. Wosnitza, R. Wünsch, and W. Seidel, Rev. Sci. Instrum. **80**, 073102 (2009).
7. J. Hebling, K.-L. Yeh, M. C. Hoffmann, B. Bartal, and K. A. Nelson, J. Opt. Soc. Am. B **25**, B6 (2008).
8. A. Sell, A. Leitenstorfer, and R. Huber, Opt. Lett. **33**, 2767 (2008).
9. C. Manzoni, H. Ehrke, M. Först, and A. Cavalleri, Opt. Lett. **35**, 757 (2010).
10. C. Vicario, B. Monoszlai, and C. P. Hauri, Phys. Rev. Lett. **112**, 213901 (2014).
11. M. Shalaby and C. P. Hauri, Nature Commun. **6**, 5976 (2015).
12. C. Vicario, B. Monoszlai, M. Jazbinsek, S.-H. Lee, O.-P. Kwon, and C. P. Hauri, Sci. Rep. **5**, 14394 (2015).
13. C. Vicario, A. V. Ovchinnikov, O. V. Chefonov, and C. P. Hauri, "Multi-octave spectrally tunable strong-field terahertz laser," arXiv 1608.05319 (2016).
14. T. Taniuchi, S. Okada, and H. Nakanishi, J. Appl. Phys. **95**, 5984 (2004).
15. T. Satoh, Y. Toya, S. Yamamoto, T. Shimura, K. Kuroda, Y. Takahashi, M. Yoshimura, Y. Mori, T. Sasaki, and S. Ashihara, J. Opt. Soc. Am. B **27**, 2507 (2010).
16. C. Manzoni, G. Cerullo, and S. De Silvestri, Opt. Lett. **29**, 2668 (2004).
17. J. R. Danielson, A. D. Jameson, J. L. Tomaino, H. Hui, J. D. Wetzel, Y. S. Lee, and K. L. Vodopyanov, J. Appl. Phys. **104**, 033111 (2008).
18. J. Lu, H. Y. Hwang, X. Li, S. H. Lee, O.-P. Kwon, and K. A. Nelson, Opt. Express **23**, 22723 (2015).
19. G. Montemezzani, M. Alonzo, V. Coda, M. Jazbinsek, and P. Günter, J. Opt. Soc. Am. B **32**, 1078 (2015).